

FUSION D+T AND D+D PRODUCTS DYNAMICS FOR THE DIFFERENT FUELING SCENARIOS IN TOROIDAL MAGNETIC REACTORS

A.V. EREMIN¹, A.A. SHISHKIN^{1,2}

UDC 621.039.623
©2008

¹V.N. Karazin Kharkiv National University
(4, Svobody Sq., Kharkiv 61077, Ukraine; e-mail: alex.eremin@gmail.com),

²Institute of Plasma Physics,
National Scientific Center "Kharkiv Institute of Physics and Technology"
(1, Akademichna Str., Kharkiv 61108, Ukraine)

Achieving the fusion power in Joint European Torus (JET) tokamak in the operation with the deuterium and tritium mixture plasma and the possible next step in the controlled fusion device International Tokamak Experimental Reactor (ITER) stimulate the further study of the fusion plasma in a toroidal magnetic trap of the reactor grade. Among many problems, there is a problem on the effect of heating injection and the different fueling scenarios on the power and particle balances of fusion plasma [1–4]. Minimization of power injection is considered in a lot of works (for example, see [1]). In this work, we would like to accent how the different fueling scenarios can lead to more optimal operation scenarios of the fusion reactor, including ITER. In our study, we use the system of balance equations [2,3] which is modified here with the time variation of particle fueling scenarios including not only fluctuations. We apply this system for the analysis of the D+T fusion products evolution in time in the tokamak reactor ITER and the D+D fusion products evolution in time in the torsatron/heliotron Large Helical Device [4–8]. There exist the analyses of plasma parameters in a fusion reactor for a steady state (see, e.g. [9]) and the temporal evolution of plasma parameters on the way (access) to ignition [10]. In this work, we develop this approach further.

1. Power and Particle Balance Equations Set for D+T Case

The following system of equations is used to describe the temporal evolution of plasma parameters averaged over the volume (the density of deuterium ions \bar{n}_D , density of tritium ions \bar{n}_T , density of thermal alpha-particles \bar{n}_α , plasma energy \bar{W} , and density of impurity ions \bar{n}_Z with charge number Z):

$$\frac{d\bar{n}_D}{dt} = S_D - \bar{n}_D \bar{n}_T \langle \sigma v \rangle_{DT} - \frac{\bar{n}_D}{\tau_p}, \quad (1)$$

$$\frac{d\bar{n}_T}{dt} = S_T - \bar{n}_D \bar{n}_T \langle \sigma v \rangle_{DT} - \frac{\bar{n}_T}{\tau_p}, \quad (2)$$

$$\frac{d\bar{n}_\alpha}{dt} = \bar{n}_D \bar{n}_T \langle \sigma v \rangle_{DT} - \frac{\bar{n}_\alpha}{\tau_\alpha}, \quad (3)$$

$$\frac{d\bar{W}}{dt} = \frac{P_{\text{ext}}}{V} + P_{\text{oh}} + P_\alpha - P_{\text{loss}} - P_{\text{brems}} - P_{\text{sync}}, \quad (4)$$

$$\begin{aligned} \frac{d\bar{n}_Z}{dt} = & S_{\text{imp}Z} - S_{Z-1} \bar{n}_{Z-1} - (\alpha_Z + S_Z) \bar{n}_Z + \\ & + \alpha_{Z+1} \bar{n}_{Z+1} - \frac{\bar{n}_Z}{\tau_Z}. \end{aligned} \quad (5)$$

Here, $x = \frac{r}{a_{\text{pl}}}$ is the dimensionless radial variable, a_{pl} is the plasma radius, bars denote the averaging over the volume; S_D and S_T are the source terms which give us the fuel rates; τ_α , τ_p , and τ_Z are, respectively, the lifetimes of thermal alpha-particles, deuterium and tritium, and impurity ions; P_{ext} is the external heating power, V is the plasma volume, P_{oh} is the density of ohmic heating power, P_α is the power density released in the form of charged particles, P_{loss} is the plasma conduction loss power density, P_{brems} is the bremsstrahlung power density, P_{sync} is the power density of synchrotron radiation; $S_{\text{imp}Z}$ is the impurity ion source, α_{Z-1} and α_Z are the recombination rates, and S_{Z-1} and S_Z are the ionization rates. Here, only one species of impurity ions is taken into account, but the system of equations can be generalized to the case of several species of impurities.

If the plasma density \bar{n}_e is induced as

$$\bar{n}_e = \bar{n}_D + \bar{n}_T + 2\bar{n}_\alpha + Z\bar{n}_Z, \quad (6)$$

then the equation of evolution of the plasma density after the substituting of (1)–(3) takes the form

$$\frac{d\bar{n}_e}{dt} = S_{DT} - \frac{\bar{n}_D + \bar{n}_T}{\tau_p} - 2\frac{\bar{n}_\alpha}{\tau_\alpha} + Z\frac{d\bar{n}_Z}{dt}, \quad (7)$$

where $S_{DT} = S_D + S_T$.

If the plasma energy density is taken in the form

$$\bar{W} = \frac{3}{2}[(\bar{n}_D + \bar{n}_T + \bar{n}_\alpha)\bar{T}_i + \bar{n}_e\bar{T}_e + \bar{n}_Z\bar{T}_Z], \quad (8)$$

then the derivative with respect to time becomes

$$\begin{aligned} \frac{d\bar{W}}{dt} = & \frac{3}{2}\bar{T}_i\left[1 + \frac{1}{\gamma_e}\frac{d\bar{n}_e}{dt} - \frac{d\bar{n}_\alpha}{dt} + \left(\frac{1}{\gamma_Z} - Z\right)\frac{d\bar{n}_Z}{dt}\right] + \\ & + \frac{3}{2}\frac{d\bar{T}_i}{dt}\left[\left(1 + \frac{1}{\gamma_e}\right)\bar{n}_e - \bar{n}_\alpha + \left(\frac{1}{\gamma_Z} - Z\right)\bar{n}_Z\right], \end{aligned} \quad (9)$$

where $\gamma_e = \frac{\bar{T}_i}{\bar{T}_e}$ and $\gamma_Z = \frac{\bar{T}_i}{\bar{T}_Z}$.

Let us introduce the parameters

$$\begin{aligned} f_D = \frac{\bar{n}_D}{\bar{n}_e}, \quad f_T = \frac{\bar{n}_T}{\bar{n}_e}, \\ f_\alpha = \frac{\bar{n}_\alpha}{\bar{n}_e}, \quad f_Z = \frac{\bar{n}_Z}{\bar{n}_e}. \end{aligned} \quad (10)$$

Then the evolution equation of the plasma temperature takes the form

$$\begin{aligned} \frac{d\bar{T}_i}{dt} = & \frac{2}{3\left(1 + \frac{1}{\gamma_e} + f_Z\left(\frac{1}{\gamma_Z} - Z\right) - f_\alpha\right)\bar{n}_e} \times \\ & \times \left(\frac{P_{\text{ext}}}{V} + P_{\text{oh}} + P_\alpha - P_{\text{loss}} - P_{\text{brems}} - P_{\text{sync}}\right) - \\ & - \frac{2\bar{T}_i}{3\left(1 + \frac{1}{\gamma_e} + f_Z\left(\frac{1}{\gamma_Z} - Z\right) - f_\alpha\right)\bar{n}_e} \times \\ & \times \left[\left(1 + \frac{1}{\gamma_e}\right)\frac{d\bar{n}_e}{dt} + \left(\frac{1}{\gamma_Z} - Z\right)\frac{d\bar{n}_Z}{dt} - \frac{d\bar{n}_\alpha}{dt}\right]. \end{aligned} \quad (11)$$

The plasma parameter profiles after averaging over the radial coordinate are assumed [3, 4] as

$$\bar{T}_i = \frac{T_i(0)}{1 + \alpha_T}, \quad \bar{n}_e = \frac{n_e(0)}{1 + \alpha_n}, \quad \bar{n}_\alpha = \frac{n_\alpha(0)}{1 + \alpha_n}. \quad (12)$$

In our further calculations, we use the profile parameters $\alpha_n = 0.5$ and $\alpha_T = 1$.

Under the assumptions about the profiles, the equations for the plasma parameters $n_e(0)$, $T_i(0)$, and the thermal alpha-particle fraction $f_\alpha(0)$ at the center of the confinement volume transform to the following form:

$$\frac{dn_e(0)}{dt} = S_{DT}(1 + \alpha_n) - n_e(0)\left(\frac{f_D(0) + f_T(0)}{\tau_p} +$$

$$+ 2\frac{f_\alpha(0)}{\tau_\alpha}\right) + Z\frac{d\bar{n}_Z}{dt}(1 + \alpha_n), \quad (13)$$

$$\begin{aligned} \frac{df_\alpha(0)}{dt} = & n_e(0)\frac{f_D(0)f_T(0)}{1 + \alpha_n}\langle\sigma v\rangle_{DT} - \\ & - f_\alpha(0)\left(\frac{1}{\tau_\alpha} + \frac{1}{n_e}\frac{dn_e(0)}{dt}\right), \end{aligned} \quad (14)$$

$$\begin{aligned} \frac{dT_i(0)}{dt} = & \frac{\frac{2}{3}(1 + \alpha_n)(1 + \alpha_T)}{\left[1 + \frac{1}{\gamma_e} + f_Z\left(\frac{1}{\gamma_Z} - Z\right) - f_\alpha(0)\right]n_e(0)} \times \\ & \times \left(\frac{P_{\text{ext}}}{V} + P_{\text{oh}} + P_\alpha - P_{\text{loss}} - P_{\text{brems}} - P_{\text{sync}}\right) - \\ & - \frac{T_i(0)}{\left(1 + \frac{1}{\gamma_e} + f_Z\left(\frac{1}{\gamma_Z} - Z\right) - f_\alpha(0)\right)n_e(0)} \times \\ & \times \left[\left(1 + \frac{1}{\gamma_e}\right)\frac{dn_e(0)}{dt} - \frac{df_\alpha(0)}{dt} + \left(\frac{1}{\gamma_Z} - Z\right) \times \right. \\ & \left. \times (1 + \alpha_n)\frac{d\bar{n}_Z}{dt}\right]. \end{aligned} \quad (15)$$

Equation (6) transforms into the following one:

$$\bar{f}_D + \bar{f}_T + 2\bar{f}_\alpha + Z\bar{f}_Z = 1. \quad (16)$$

Now it is possible to compare this system of equations (13)–(15) with the analogous system of the evolution equations in [1]. The difference is as follows. We take into account the impurities density \bar{n}_Z under the charge neutrality condition, which implies to Z_{eff} , the alpha particles fraction. The fraction $f_\alpha(0)$ enters in the different way, which leads to the different form of the plasma energy balance equation. This is a consequence of the different form of \bar{W} taken here. We took the contribution of thermal alpha-particles into account in (8). We do not multiply the derivative $\frac{df_\alpha}{dt}$ by the coefficient of 2; the magnitude $f_\alpha(0)$ is present in the denominator of the expressions on the right-hand side of Eq. (15) for the evolution of the plasma temperature T_i . If there is the removal of thermal alpha particles (in this case, $\frac{df_\alpha}{dt} < 0$), then their contribution should lead to a decrease of the temperature T_i . However at the same time, the decrease of f_α should cause the increase of T_i , because of its presence in the denominator. So we can conclude that there are two competitive mechanisms,

and it is necessary to find the “operating windows” within which the removal of thermal alpha particles is favorable for the achieving the ignition boundary. This is done in [4].

In the following calculations, we omit the terms proportional to $\frac{dn_Z}{dt}$. The impurity ion density enters as a parameter in the bremsstrahlung power [see Eq. (21)]. In our calculations, we take f_Z equal to 1.

2. Models of D+T Fusion Product Rate, Radiation and Transport Losses

For the further analysis, we chose the following models for alpha-particle power input and the radiation and transport losses.

The reaction rate is used in the following form [9, 11]:

$$\langle \sigma v \rangle_{DT} = \frac{2.57 \times 10^{-18}}{T^{2/3} U^{5/6}} \exp\left(-\frac{19.98 U^{1/3}}{T^{1/3}}\right) \left[\frac{\text{m}^3}{\text{s}}\right], \quad (17)$$

where

$$U = 1 - T_i(0.02507 + T_i(0.00258 - 0.0000619T_i)) / (1 + T_i(0.066 + 0.00812T_i)). \quad (18)$$

From the literature, the following expression for the thermal reaction rate is well known [13]:

$$\langle \sigma v \rangle_{DT} = 3.68 \times 10^{-18} \frac{1}{T^{2/3}} \exp\left(-\frac{19.94}{T^{1/3}}\right) \left[\frac{\text{m}^3}{\text{sec}}\right], \quad (19)$$

where the temperature T is measured in keV.

Let's make some estimation for the energies releasing and outgoing from a plasma volume during the ignition and the ignited operation. We will have the alpha heating power due to fusion reactions in the plasma volume. It basically depends on the plasma density and the reaction rate $\langle \sigma v \rangle_{DT}$. Bremsstrahlung energy losses due to collisions of plasma electrons with ions mainly depend on the plasma density and the effective charge number. The power of plasma conduction losses depends on temperature and has a strong inverse dependence on the effective energy confinement time. The quantity P_{incoming} is the sum of all incoming powers, like fusion power and auxiliary heating power.

The alpha-particle power is calculated by the expression

$$P_\alpha = 5.6 \times 10^{-13} n(0)^2 f_D f_T \langle \sigma v \rangle_{DT} \left[\frac{\text{W}}{\text{m}^3}\right], \quad (20)$$

and the bremsstrahlung power P_{brems} is given as

$$P_{\text{brems}} = 5.4 \times 10^{-37} Z_{\text{eff}} n(0)^2 \sqrt{T_e(0)} \left[\frac{\text{W}}{\text{m}^3}\right]. \quad (21)$$

Here, we calculate the effective charge state as follows:

$$Z_{\text{eff}} = \frac{1}{n(0)} \sum_Z n_Z(0) Z^2. \quad (22)$$

The plasma conduction loss power P_{loss} is given as follows:

$$P_{\text{loss}} = \frac{3}{2} \times 1.6 \times 10^{-19} (1 + f_D + f_T) \frac{n(0)T(0)}{\tau_E} \left[\frac{\text{W}}{\text{m}^3}\right], \quad (23)$$

where the temperature $T_{i,e}(0)$ is measured in keV, and the density $n(0)$ in $[\text{m}^{-3}]$. Profile parameters are not shown here, but they are taken in the account in numerical calculations.

The thermal reaction rate $\langle \sigma v \rangle_{DT}$ is a key parameter which defines the fusion power density released in the high-temperature D+T plasma. There is a minimum on the $U(T)$ function, as a result of which we have inflection on the energy dependence curve of alpha particles. Here, we can see a simple dependence between the effective energy confinement time and the conductive losses in the fusion plasma. The greater is τ_E , the smaller the conductive losses power density in the plasma. As a result, we get a better confinement of energy in the fusion plasma volume.

Bremsstrahlung losses from plasma are more than twenty times smaller than conductive losses in non dusty plasma with effective charge number up to 5. But with increase in the effective charge number due to the presence of a heavy high-charge impurity in plasma, we will get a rapid increase of the bremsstrahlung power density.

We have the second-power dependence of the effective charge number on bremsstrahlung power losses, which means that the introduction of impurities with Z of about 10 leads to the about two-order increase in bremsstrahlung power losses.

The confinement time τ_E can be estimated by the ITER98P scaling

$$\tau_E^{\text{ITER98P}} = 0.0365 M^{0.2} I_p^{0.97} R^{1.93} (a/R)^{0.23}$$

$$k_{\text{elongation}}^{0.67} (n_0 \times 10^{-19})^{0.41} B_t^{0.08} P_{\text{heat}}^{-0.63}, \quad (24)$$

where M is measured in atom mass units, plasma current I_p – in MA, major plasma radius R – in meters,

$k_{\text{elongation}}$ – plasma elongation, plasma density n in m^{-3} , magnetic field in T, P_{heat} external heating in MW. In our calculations, we take τ_E equal to 1.8 sec [3] and use the relations $\tau_p = 10\tau_E, \tau_\alpha = 10\tau_E, \gamma_e = 1$. We neglect the impurity ion temperature effect, and so γ_Z is taken equal to zero, $f_D = f_T = \frac{1-2f_\alpha}{2+8f_Z}$.

3. Plasma Parameter Evolution Under Different Fueling Scenarios for D+T Case in Tokamak Reactor

In the present work, we obtain the dependence of the plasma ignition boundary on such plasma parameters as the density, temperature, fraction of alpha-particles, and operation path (the time evolution of the plasma parameters $n_e(0)$ and $T_i(0)$) for different ignition regimes. The careful control of the plasma density by fuelling S_{DT} is necessary. Real time measurements of the plasma density and the ion temperature during the heating phase are needed to get the desirable operating point on the $n - T$ plane (POPCON). The thermally stable ignition regime can be reached by controlling the alpha particles fraction f_α and the plasma ion temperature T_i . If the helium ash confinement time changes, then the helium ash density and the plasma density change together. Without diagnostics of which plasma parameters, like the helium ash fraction or energy confinement time, are changed during the ignition and the ignited operation, it's easier to operate the plasma ignition path by the feedback control of the heating power and the fuelling of deuterium and tritium by monitoring the fusion power.

It also possible to control the ignition process by changing Z_{eff} in plasma due to the injection of an impurity pellet, which increases bremsstrahlung power losses P_{brems} and leads to a slower plasma temperature increase during the ignition.

On the plasma operation graphs, Fig 1,*a,c* and Fig. 1,*b,d*, we present the simulation results for fueling and input power different scenarios. Basically, the following difference can be noted: for the Fig. 1,*b,d* we have a lower D+T fueling rate than that for the Fig. 1,*a,c*.

Auxiliary heating powers in both series are equal. Such fueling scenario has a strong influence on the destination plasma parameters. Due to this, we have the steady-state temperature for the first fueling scenario of about 5 keV higher than that for the second one.

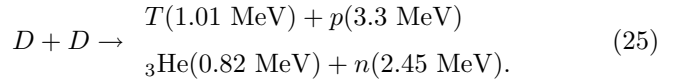
Let's take a look on the plasma operation path with different fueling source operations scenarios. Figures 1,*a,c* and 1,*b,d* present the temporal evolution of the

plasma density, alpha ash fraction f_α (in tens of percents), and plasma temperature T_i (tens of keV) for different fueling scenarios.

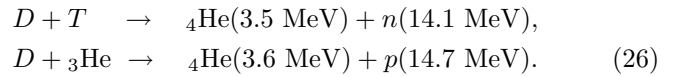
The operation paths (plasma density versus plasma temperature) on the background of the POPCON (Fig. 2) show us the consequence of the stages of plasma heating and density increase due to the fuel coming and heating. It is easy to note that the operation paths under different fuelling scenarios reach the ignition region in different ways. A smaller value of S_{DT} causes the operation path position to be placed on the $n - T$ plane at smaller values of plasma density and temperature. This means that we need a less external power and can operate in the region of lower densities. So we can use a simpler fuel and power injection system under the easier plasma operation.

4. Power and Particle Balance Equations Set for D+D Case

We study the following fusion plasma processes in Large Helical Device:



There are two channels for the reaction with almost equal probability. There is a possible secondary reaction of D plasma with D+D fusion products $T(1.01 \text{ MeV})$ and ${}_3\text{He}(0.82 \text{ MeV})$ with higher fusion rate:



In our numerical model, we take into account primary and secondary reactions. In the secondary reaction process, we neglect the difference in the products energies and assume that we have one reaction with the same reaction rate and products with averaged energies.

The following system of equations is used to describe the temporal evolution of the plasma parameters such as the density of source deuterium plasma ions \bar{n}_D , density of thermal fusion products $\bar{n}_{T,3\text{He}}$ (tritium and helium-3), and plasma energy \bar{W} :

$$\begin{aligned} \frac{d\bar{n}_D}{dt} &= S_D - \bar{n}_D^2 \langle \sigma v \rangle_{DD(p,n)} - \frac{\bar{n}_D}{\tau_D} - \\ &- \bar{n}_D \bar{n}_{T,3\text{He}} \langle \sigma v \rangle_{D-T,3\text{He}}, \end{aligned} \quad (27)$$

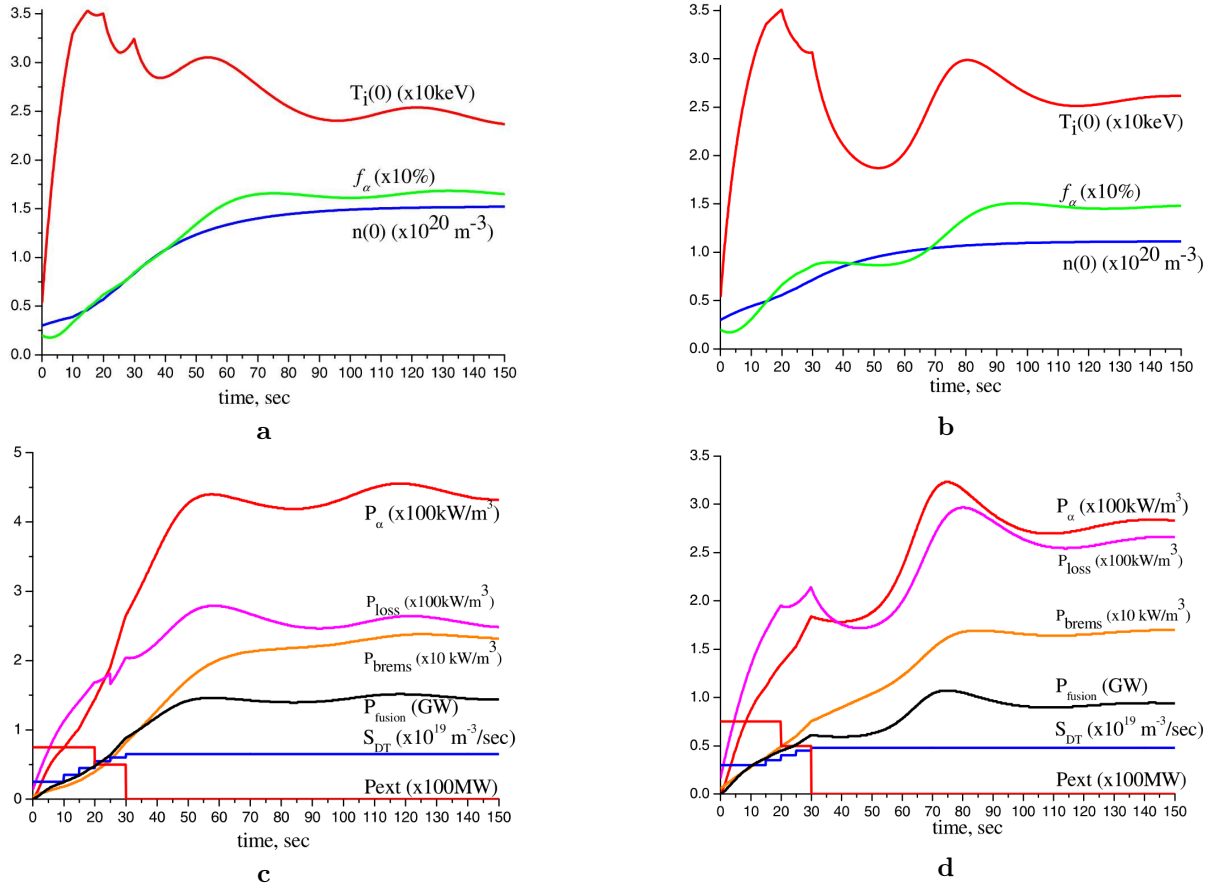


Fig. 1. Temporal evolution of the plasma parameters in the ITER D+T fusion reaction: *a* – n, f_α, T_i for the fueling power $P_{\text{ext}} = 50 \div 75$ MW and the fueling source density $S_{DT} = (0.25 \div 0.65) \times 10^{19} \text{ m}^{-3}\text{s}^{-1}$, *b* – n, f_α, T_i for the fueling power $P_{\text{ext}} = 50 \div 75$ MW and the fueling source density $S_{DT} = (0.3 \div 0.5) \times 10^{19} \text{ m}^{-3}\text{s}^{-1}$, *c* – $P_{DT}, P_{\text{loss}}, P_{\text{brems}}, P_{\text{fusion}}, S_{DT}, P_{\text{ext}}$ for $S_{DT} = (0.25 \div 0.65) \times 10^{19} \text{ m}^{-3}\text{s}^{-1}$, *d* – $P_{DT}, P_{\text{loss}}, P_{\text{brems}}, P_{\text{fusion}}, S_{DT}, P_{\text{ext}}$ for $S_{DT} = (0.3 \div 0.5) \times 10^{19} \text{ m}^{-3}\text{s}^{-1}$

$$\frac{d\bar{n}_{T,3\text{He}}}{dt} = \bar{n}_D^2 \langle \bar{\sigma v} \rangle_{DD} - \bar{n}_D \bar{n}_{T,3\text{He}} \langle \bar{\sigma v} \rangle_{D-T,3\text{He}} - \frac{\bar{n}_{T,3\text{He}}}{\tau_{T,3\text{He}}}, \quad (28)$$

$$\frac{d\bar{W}}{dt} = \frac{P_{\text{ext}}}{V} + P_D - P_{\text{brems}} - \frac{3}{2} \frac{\bar{n}_D \bar{T}_D}{\tau_E}. \quad (29)$$

Here, $x = r/a_{\text{pl}}$ is the dimensionless radial variable, a_{pl} is the plasma radius, bars denote the averaging over the volume; S_D is the source term which gives us the fuel rate, $\tau_D, \tau_{T,3\text{He}}$ are the particle confinement times: the deuterium τ_D, T and ^3He fusion products ($\tau_{T,3\text{He}}$). We assume that P_{ext} is the external heating power, V is the plasma volume, P_D is the power density released in the form of charged particles, P_{loss} is the plasma conduction loss power density ($P_{\text{loss}} = \frac{3}{2} \frac{\bar{n}_D \bar{T}_D}{\tau_D}$), P_{brems} is the bremsstrahlung power density. All three heating

schemes are taken into account as $P_{\text{ext}} = P_{\text{ICRF}} + P_{\text{ECH}} + P_{\text{NBI}}$ with the time dependence written below. We use the system of evolution equations (3)–(5), as it was described in [1, 6]

5. Model of D+D Fusion Product Rate and Transport Losses in Large Helical Device

The reaction rate for the D+D fusion reaction is used in the following form [13]:

$$\langle \bar{\sigma v} \rangle_{DD} = 2.33 \times 10^{-20} \frac{1}{T^{2/3}} \exp\left(-\frac{18.76}{T^{1/3}}\right) \left[\frac{\text{m}^3}{\text{s}}\right], \quad (30)$$

where the temperature T is measured in keV.

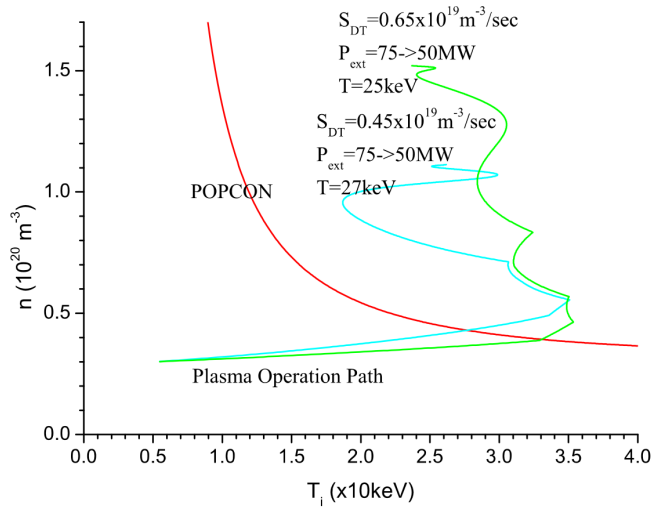


Fig. 2. Operation path (plasma density versus plasma temperature) on the background of the POPCON

Let's make some estimation for the energies releasing and outgoing from a plasma volume during the ignition and the ignited operation. We have the particles heating power due to fusion reactions in the plasma volume. It basically depends on the plasma density and the reaction rate $\langle \sigma v \rangle_{DD}$. Bremsstrahlung energy losses due to collisions of plasma electrons with ions mainly depend on the plasma density and the effective charge number. The plasma conduction losses power depends on the temperature and has a strong inverse dependence on the effective energy confinement time. The quantity P_{incoming} is the sum of all incoming powers, like the fusion power and auxiliary heating power.

We calculated the power releasing in the form of charged particles due to fusion processes in plasma by the expression

$$P_D = 3.3 \times 10^{-13} n_D^2 \langle \sigma v \rangle_{DD} \left[\frac{\text{W}}{\text{m}^3} \right], \quad (31)$$

the bremsstrahlung power P_{brems} by formula (21), and the effective charge state by formula (22).

The plasma conduction loss power P_{loss} is given as following:

$$P_{\text{loss}} = \frac{3}{2} \times 1.6 \times 10^{-19} \frac{(n(0) + n_{p+n}(0))T(0)}{\tau_E} \left[\frac{\text{W}}{\text{m}^3} \right], \quad (32)$$

where the temperature $T_{i,e}(0)$ is measured in keV, and the density $n(0)$ in $[\text{m}^{-3}]$.

The thermal reaction rate $\langle \sigma v \rangle_{DD}$ is a key parameter which defines the fusion power density released in a high-temperature fusion plasma. We have to note that it's

much easier to get the steady ignited operation in a low-temperature region for D+D plasma. The reason for it is a very rapid increase of conduction power density losses in the confinement volume with temperature. But the power release due to fusion processes in plasma is many times smaller than losses, because the thermal reaction rate for the D+D reaction is too small in the reachable temperature region.

Here, we can see the simple dependence between the effective energy confinement time and the conductive losses in fusion plasma. The greater is τ_E , the smaller the conductive losses power density in plasma. As a result, we get a better confinement of energy in the fusion plasma volume. At the present time, it is possible to get the energy confinement time on Large Helical Device up to $\tau_E = 0.36$ s.

Bremsstrahlung losses from plasma are more than twenty times smaller than conductive losses in a plasma with effective charge number up to 5. But with increase in the effective charge number, which means the presence of a heavy high-charge impurity in plasma, we will get a rapid increase of the bremsstrahlung power density. We have the strong dependence of bremsstrahlung power losses on the effective charge number, which means that the introduction of impurities with Z of about 10 leads to the about two-order increase of bremsstrahlung power losses.

The energy confinement time τ_E of about 1 sec demonstrates a desirable level of power losses. Due to different dependences of the incoming and outgoing powers from plasma, we have to understand that we need to find such operation region, where we have optimal values of each dependence.

The confinement time τ_E is estimated by the international ISS95 stellarator scaling [12]:

$$\tau_E^{\text{ISS95}} = 0.0079 a^{2.21} R^{0.65} P_{\text{heat}}^{-0.59} (n_0 \times 10^{-19})^{0.51} B_t^{0.83} t_{2/3}^{0.4}, \quad (33)$$

where major plasma radius R – in m, plasma density n in m^{-3} , magnetic field in T, P_{heat} external heating in MW. In our following calculations, we take τ_E equal to 0.36 s [12].

6. Plasma Parameter Evolution Under Different Fueling Scenarios for D+D Case in Large Helical Device

The numerical calculations for different fueling and power injection scenarios were aimed to obtain optimal regions of the plasma operation. We have studied the

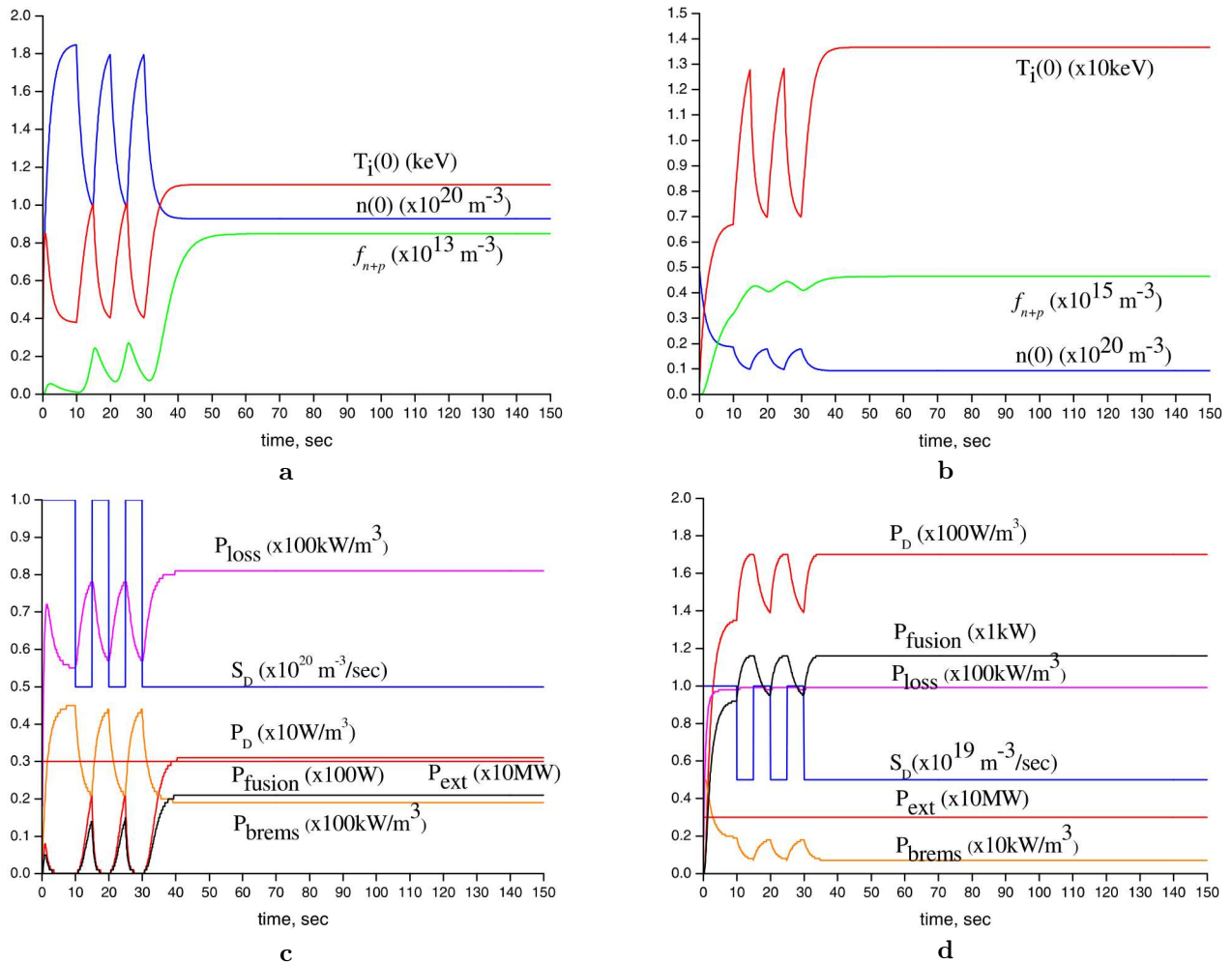


Fig. 3. Temporal evolution of the plasma parameters in the Large Helical Device D+D fusion reaction: *a* – (n, f_{α}, T_i) for $P_{\text{ext}} = 3$ MW and the fueling power density $S_D = 0.5 \times 10^{20} \text{ m}^{-3}\text{s}^{-1}$ with steady state operation, *b* – (n, f_{α}, T_i) for $P_{\text{ext}} = 3$ MW and the fueling power density $S_D = 0.5 \times 10^{19} \text{ m}^{-3}\text{s}^{-1}$ with steady state operation, *c* – ($P_D, P_{\text{loss}}, P_{\text{brems}}, P_{\text{fusion}}, S_D, P_{\text{ext}}$) for the fueling power density $S_D = 0.5 \times 10^{20} \text{ m}^{-3}\text{s}^{-1}$, *d* – ($P_D, P_{\text{loss}}, P_{\text{brems}}, P_{\text{fusion}}, S_D, P_{\text{ext}}$) for the fueling power density $S_D = 0.5 \times 10^{19} \text{ m}^{-3}\text{s}^{-1}$

influence of different fueling scenarios on steady state parameters, modeled the evolution of plasma parameters (plasma density, temperature, fusion products rate) with different fueling scenarios of the removal of products, and investigated the steady state operation under the different density fueling and power injection schemes.

We observe the fusion D+D plasma operation for 150 sec, which is long enough for the steady state operation establishment. It was shown in the previous investigations that a steady state established for such a period stays stable in future. Thus, such a period of the plasma observation is enough indicative. This does not too simplify the model and, on the other hand, does not result in a significant growth of the numerical solution time for the system of evolution equations.

In our model, we consider that fuel goes to the confinement volume by the periodic injection of deuterium pellets in plasma and assume the uniform distribution of injected particles and the heating power at the plasma center and on the periphery. Thus, on the numerical solution of the system of equations describing the time evolution of the plasma parameters, we did not consider differences in the profiles of the fuel density and temperatures, due to their nonhomogeneity in various regions of plasma. We assumed that the distributions of injected fuel and power are isotropic over the total plasma volume.

The results of numerical calculations of the above-stated system of equations describing the time evolution of plasma parameters are given in Figs. 3 and 4. In

Fig. 3,*a,b*, we represent the density of the basic plasma $n(0)$ in m^{-3} and the density of fusion products f_{n+p} (T and ${}^3\text{He}$) formed as a result of the thermonuclear D+D reaction.

On the second series of each graph, the initial plasma parameters (the injected density of source fuel ions S_D in $\text{m}^{-3}\text{s}^{-1}$ and the power of external heating of plasma P_{ext} in W) are given. In Fig. 3,*c,d*, we show the results of numerical modeling for all power densities allocated in plasma: thermonuclear fusion P_D , density of energy leaving plasma due to bremsstrahlung losses P_{brems} in W/m^3 , plasma conductivity losses P_{loss} in W/m^3 , and total thermonuclear power allocated in the whole volume of the experimental device P_{fusion} in W.

Let's examine the behavior of plasma at initial parameters and the structure of input power and fuel in the case corresponding to graphs in Fig.3. Our purpose in this case is to reach the basic plasma density high enough, the higher ratio of D+D fusion products in plasma, and temperature of the basic plasma up to 10 keV. For this purpose, we use the high density of particles introduced in plasma $S_D = 1 \times 10^{19} \text{ m}^{-3}\text{s}^{-1}$ and the power density entered into plasma of the order 3 MW/s. Such an input of the initial parameters enables us to avoid the level of losses in plasma, when they would considerably exceed a positive effect given due to the contribution of the energy of fusion products and a power injected from the outside. The smooth escalation of the input density from 0.6×10^{19} to $1 \times 10^{19} \text{ m}^{-3}\text{s}^{-1}$ at the initial stage of ignition at a constant power of external heating allows us to obtain the significant jump of the plasma temperature in time at the initial stage of ignition due to a high concentration of energy in the plasma volume.

We would like to note that the input of fuel particles (source term S_D) in the form of "steps in time" (Fig. 3,*c,d*) gives us the opportunity to slowly decrease the plasma energy per density unit. As a result of such injection scheme of particles, we get lower parameters, more effective heating, and the optimum ratio for incoming and outgoing powers from the experimental device.

7. Effect of the Use of the Analytical Expression for Confinement Time τ_E Instead of τ_E Scaling

In spite of that fact, the use of τ_E in the form of scaling is wide-spread [1, 3] and [14, 15]. There exists also the analysis of the plasma access to ignition with

the analytical expression of τ_E with a dependence on temperature and density (see, e.g., [2]). Here, we assume the physical mechanism of transport which appropriates to the neoclassical plateau regime.

We assume the next expression for τ_E in a plasma confinement volume for the plateau case:

$$\tau_E^{\text{plateau}} = 9.4 \times 10^4 \frac{a_{\text{pl}}^2 R B^2 \iota}{M^{1/2} T^{3/2}}. \quad (34)$$

From the comparison of Fig. 4 and Fig. 1,*b,d*, it is easy to see that the transition from τ_E scaling to τ_E^{plateau} by the lifetime in the analytical form [see Eq.(34)] causes additional fluctuations of parameters of plasma, but the steady state is established finally. The plasma parameters appear approximately similar in two considered cases. The energy exhausted in the form of charged particles appears above up to 1.5 times, and the thermonuclear power P_{fusion} allocated in the confinement volume appears proportionally above. The bremsstrahlung power P_{brems} also appears greater by 1.5 times than that in the case without taking into account the analytical dependence of τ_E .

8. Conclusions

1. We have established the effect of a change of the fuel source S_{DT} in time on the plasma parameters in the steady state. We should note that, in the case of a smaller fuel rate (Fig. 1), the steady state is formed on the level of the lower value of the helium ash (approximately 12 % see Fig. 1,*a,c*) instead of 15 % (Fig. 1,*b,d*). The fusion power is somewhat smaller, namely $P_{\text{fusion}} \approx 1 \text{ GW}$ in the case of the smaller fuel rate (Fig. 1,*d*) in comparison with the $P_{\text{fusion}} \approx 1.5 \text{ GW}$ in the previous case (Fig. 1,*c*).

2. Plasma operation paths (the temporal evolution of plasma parameters $n_e(0)$ and $T(0)$) on the background of POPCON line (see Fig. 2) can distinguish noticeably under the different scenarios of fueling. The plasma operation path for $S_{DT} = 0.45 \times 10^{19} \text{ m}^{-3}\text{s}^{-1}$ in Fig. 2 leads to lower values of the temperature $T(0)$ and the plasma density $n_e(0)$ under the desired value of the output fusion power P_{fusion} .

3. It is shown in Fig. 4 that, on Large Helical Device, we can get fusion products with the density $f_{np} = 0.8 \times 10^{13} \text{ m}^{-3}$ for the next operating parameters: the external heating power of 3 MW, source fueling density $S_D = 0.5 \times 10^{20} \text{ m}^{-3}\text{s}^{-1}$, ion's temperature $T = 1.1\text{keV}$, and plasma density $n = 1 \times 10^{20} \text{ m}^{-3}$. For another fueling and heating scheme (source fueling

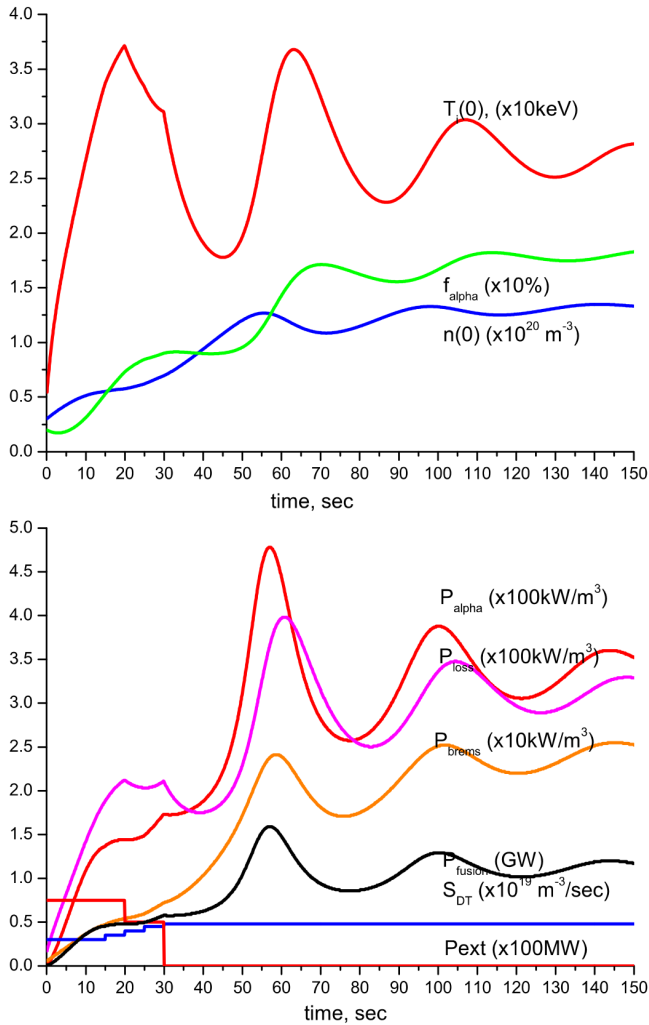


Fig. 4. Temporal evolution of plasma parameters in the ITER D+T fusion reaction for the analytical dependence τ_E^{plateau} case: the 1st graph – n, f_α, T_i for the fueling power $P_{\text{ext}} = 50 \div 75$ MW and the fueling source density $S_{DT} = (0.3 \div 0.5) \times 10^{19} \text{ m}^{-3}\text{s}^{-1}$; the 2nd graph – $P_{DT}, P_{\text{loss}}, P_{\text{brems}}, P_{\text{fusion}}, S_{DT}, P_{\text{ext}}$ for $S_{DT} = (0.3 \div 0.5) \times 10^{19} \text{ m}^{-3}\text{s}^{-1}$

density $S_D = 0.5 \times 10^{19} \text{ m}^{-3}\text{s}^{-1}$, ion temperature $T = 13$ keV, plasma density $n = 1 \times 10^{19} \text{ m}^{-3}$, the density of fusion products $f_{np} = 0.4 \times 10^{15} \text{ m}^{-3}$ is obtained. Such results take place for the steady state plasma operation regime and are observed for the 150-sec period. Nowadays, there is a technical possibility to inject the 3-MW heating power into the confinement volume on Large Helical Device.

4. The use of the analytical expression for the confinement time τ_E instead of the τ_E scaling causes additional fluctuations of plasma parameters, but the steady state is finally established with the parameters

similar to those for the τ_E scaling. Here, we restrict ourselves with the transport model of the neoclassical plateau regime. A more detailed study will be presented elsewhere.

This work is partly supported in the framework of the Science and Technology Center in Ukraine, Project No.3685. The authors express their gratitude to Professor K.N. Stepanov, Professor I.O. Girka, Doctor I.V. Pavlenko, and Professor V.D. Yegorenkov for useful discussions and comments.

1. O. Mitarai, A. Sagara, H. Chikaraishi, S. Imagawa, K. Watanabe, A.A. Shishkin, and O. Motojima, Nuclear Fusion **47**, 1411 (2007).
2. E. Rebhan and U. Vieth, Nuclear Fusion **37**, 251 (1997).
3. O. Mitarai and K. Muraoka, Nuclear Fusion **37**, 1523 (1997).
4. A.V. Eremin and A.A. Shishkin, J of Kharkiv Univ., Phys. Ser. "Nuclei, Particles, Fields" **3**, 62 (2007).
5. A.A. Shishkin, O. Motojima, S. Sudo, A.V. Eremin, A.A. Moskvitin, and Yu.K. Moskvitina, Fusion Engineering & Design, **81**, 2733 (2006).
6. O. Motojima, N. Ohya, A. Komori, N. Noda, K. Yamazaki, H. Yamada, and A. Sagara, Plasma Physics and Controlled Fusion **38**, A72 (1996).
7. O. Motojima, K. Ida, K.Y. Watanabe, Y. Nagayama, A.Komori, T. Morisaki, and B.J. Peterson, Nuclear Fusion **45**, S255 (2005).
8. O. Motojima, H. Yamada, A. Komori, N. Ohya, T. Mutoh, O. Kaneko, and K. Kawahata, Nuclear Fusion **47**, S668 (2007).
9. C.D. Beidler, E. Harmeyer, J. Kisslinger, I. Ott, F. Rau, and H. Wobig, Max-Planck-Institut fur Plasmaphysik **2**, 318 (1993).
10. A. Perez-Navarro, Max-Planck-Institut fur Plasmaphysik **2**, 331 (1996).
11. H.S. Bosch and G.M. Hale, Nuclear Fusion **32**, 611 (1992).
12. U. Stroth, M. Murakami, R.A. Dory, H. Yamada, S. Okamura, F.Sano, and T. Obiki, Nuclear Fusion **36**, 1063 (1996).
13. J.D. Huba, NRL PLASMA FORMULARY, Beam Physics Branch Plasma Physics Division Naval Research Laboratory Washington, DC 20375. 45 (2007).
14. O. Mitarai, A. Oda, A. Sagara, K. Yamazaki, and O. Motojima, Fusion Engin. and Design **70**, 247 (2004).
15. E.J. Vitela and J.J. Martinell, J. Plasma Fusion Res. SERIES **3**, 517 (2000).

ДИНАМІКА ПРОДУКТІВ ТЕРМОЯДЕРНОГО
СИНТЕЗУ D+T ТА D+D ДЛЯ РІЗНИХ
СЦЕНАРІЇВ УВЕДЕННЯ ПАЛИВА
В ТОРОЇДАЛЬНИХ ПАСТКАХ
З МАГНІТНИМ УТРИМАННЯМ

О.В. Єрємін, О.О. Шішкін

Резюме

Отримання термоядерної потужності на пристроях JET при роботі з дейтерієво-тритієвою сумішшю, а також майбутній експеримент з керованого термоядерного синтезу D+T на ITER стимулюють розвиток подальших досліджень термоядерної плазми в тороїдальних магнітних пастках реакторного масштабу. Поряд з безліччю завдань у цій області існує також невирішене питання щодо впливу схеми введення по-

тужності та різних сценаріїв подачі палива на баланс енергії й частинок у термоядерній плазмі [1–4]. Подібні дослідження, присвячені мінімізації потужності, що вводиться, розглядаються в ряді робіт (див., наприклад, [1]). У цій роботі зроблено акцент на вивченні того, який саме сценарій введення палива може привести до найбільш оптимальних сценаріїв роботи термоядерного реактора, зокрема ITER. Для розгляду використовується система рівнянь балансу [2, 3], модифікована з урахуванням зміни в часі сценаріїв введення частинок в об'єм реактора. Розгляд проведено для еволюції продуктів синтезу D+T на токамаці ITER, а також продуктів термоядерної реакції D+D на торсатроні LHD [4–8]. Відомі різні дослідження параметрів плазми в термоядерному реакторі для досягнення стаціонарного режиму горіння (див., наприклад, [9]) і часової еволюції параметрів плазми на шляху до області горіння [10]. У цій роботі наведено подальший розвиток такої моделі.